

A Combined Phase and Force Compensation Method for Real-time Hybrid Testing

Pei-Ching Chen, & Keh-Chyuan Tsai

National Taiwan University, Taiwan

National Center for Research on Earthquake Engineering, Taiwan



SUMMARY:

Real-time hybrid testing is an advanced method for examining the dynamic responses of structures under seismic loading. An inevitable time-delay between the desired and measured displacements would lead to incorrect test results. Therefore, delay compensation is critical for real-time hybrid testing. In this paper, a dual compensation strategy is proposed by a combination of a phase-lead compensator (PLC) and a restoring force compensator (RFC). The PLC is formulated by using weighted linear extrapolation and inverse model principle. In addition, the gradient adaptive law is adopted to estimate the time delay and adjust the PLC during a test. On the other hand, the RFC is based on the equilibrium of the equation of motion considering the tracking error between the desired and the measured displacements. The computed compensation force is fed back to correct the structural response. The feasibility of the proposed strategy is demonstrated through analytical simulations and experimental studies.

Keywords: real-time hybrid testing, delay compensation, adaptive law

1. INTRODUCTION

Real-time hybrid testing method is a versatile technique for evaluating the dynamic responses of structures subjected to earthquake ground motions. During a hybrid simulation test, the equations of motion are solved using a step-by-step integration scheme. In most cases, the inertia and damping forces are analytically modelled and the restoring force is measured from the test structure. Inevitably, there is a small but significant enough delay between the command displacement and the achieved displacement due to the dynamics of the servo-hydraulic systems. The effect of actuator delay can be viewed as introducing negative damping to the structural system (Horiuchi *et al.* 1999). It would result in inaccurate test results or even destabilize the overall structural system. As a result, several delay compensation methods have been investigated to solve the unstable problems due to delay (Zhao *et al.* 2003; Jung and Shing 2006; Chen and Ricles 2009). Generally, they can be classified into two types: (1) to predict the command in advance; and (2) to implement an outer-loop digital delay compensator. The delay compensators are based on a known constant actuator delay during real-time hybrid tests; however, researchers have indicated that when the stiffness increases the time delay also increases (Darby *et al.* 2002). Therefore, methods for estimating the actuator delay during real-time hybrid tests have been developed and considered essential (Darby *et al.* 2002; Ahmadizadeh *et al.* 2008).

In this paper, a dual-compensation strategy is proposed to achieve more stable and accurate experimental results of real-time hybrid testing. It includes an adaptive second-order phase lead compensator (PLC) and an online restoring force compensator (RFC). The servo-hydraulic system is modelled by using weighted linear extrapolation between the command and the measured displacements. Then the PLC is formulated by applying the inverse model principle. In addition, the gradient adaptive law is adopted to estimate the actuator delay in the format of parametric model. On the other hand, the RFC is based on the equilibrium of the equation of motion considering the tracking error between the desired and the measured displacements. A moving-averaged tangent stiffness is calculated online and used to compute the RFC at each step. The compensation force is then fed back to the equation of motion to correct the structural response. The feasibility of the proposed dual

compensation strategy is examined through several analytical simulations in which the structure is a lightly-damped and short-period single-degree-of-freedom (SDOF) building. Finally, the dual compensation strategy is validated by conducting real-time hybrid tests of an SDOF portal frame using a dynamic shaking table. The test results are compared with an assumed exact analytical solution to demonstrate the effectiveness of the proposed compensation strategy.

2. PHASE LEAD COMPENSATOR

2.1. Phase lead compensator in discrete format

For displacement-controlled testing systems, the transfer function from the command to the achieved displacements in frequency domain can be approximated using a first-order transfer function (Zhao *et al.* 2003). The system performance can be improved by tuning up the proportional gains such that the roll-off frequency is larger than the specific frequency range of interest. Therefore, the servo-hydraulic system can be treated as a pure time delay system if the roll-off frequency is far from the structural vibration frequency. In other words, there would be small but negligible amplitude error between the measured and desired displacements. The servo-hydraulic actuators are mostly driven by the digital controller in the laboratory. Hence, the phase lead compensator are designed and analyzed in discrete-time. Generally, the discrete transfer function $G(z)$ of a linear discrete-time system can be expressed as:

$$G(z) = \frac{b_m z^m + b_{m-1} z^{m-1} + \dots + b_1 z + b_0}{a_n z^n + a_{n-1} z^{n-1} + \dots + a_1 z + a_0} \quad (2.1)$$

where a_n, \dots, a_0 and b_n, \dots, b_0 are the coefficients in the denominator and the numerator, respectively. The parameter z is a complex number in the z domain. If the number $n \geq m$, the system is called a causal system, which means the output depends only on the past and current inputs. Performing the z transformation, the transfer function of a pure time delay system in discrete time is z^{-k} , where k is the number of the delay steps. If the inverse compensation method is used to design the compensator, its transfer function in the z domain is z^k , which is not causal because the output depends on the future input. Consequently, a simplification of the discrete time delay system is crucial.

Consider a discrete pure time delay system with a delay time $\alpha \Delta t$, where α is an integer greater than 0 and Δt is the sampling period of the discrete system. The relation between the $(n+1)$ th step measured displacement $x_m[n+1]$, and the n th step measured displacement $x_m[n]$ can be simplified as a weighted linear extrapolation:

$$x_m[n+1] = x_m[n] + slope \cdot \Delta t = x_m[n] + \frac{x_{avgc}[n] - x_{avgm}[n]}{\alpha \Delta t} \cdot \Delta t \quad (2.2)$$

in which the n th averaged command displacement $x_{avgc}[n]$ and the averaged measured displacement $x_{avgm}[n]$ are:

$$x_{avgc}[n] = \frac{W_1 x_c[n+1] + W_2 x_c[n] + x_c[n-1]}{W_1 + W_2 + 1} \quad (2.3)$$

$$x_{avgm}[n] = \frac{W_1 x_m[n+1] + W_2 x_m[n] + x_m[n-1]}{W_1 + W_2 + 1} \quad (2.4)$$

where $x_c[n-1]$, $x_c[n]$, and $x_c[n+1]$ are the command displacements at the $(n-1)$ th, n th, and $(n+1)$ th step, respectively. The parameter $x_m[n-1]$ is the $(n-1)$ th step measured displacement. The variables W_1 and W_2 are the weightings. The discrete PLC, $C(z)$, can be directly obtained by applying the z -transform to Eqn. 2.2 and the inverse model principle. It can be expressed as:

$$C(z) = \frac{[W_1 + (W_1 + W_2 + 1)\alpha]z^2 + [W_2 - (W_1 + W_2 + 1)\alpha]z + 1}{W_1 z^2 + W_2 z + 1} \quad (2.5)$$

It is noted that the orders of the denominator and the numerator of the derived second-order PLC must be identical when the inverse compensation method is adopted. Otherwise, the PLC would become non-causal and impractical in real application. Furthermore, the roots in the denominator (poles) of the PLC must be located inside a unit circle in the z -domain to ensure it is realizable and stable. Applying the condition that the poles must be bounded inside a unit circle, the stable regions of W_1 and W_2 can be obtained as shown in Fig. 2.1. Once the delay time $\alpha\Delta t$ is known, the designer can choose any W_1 and W_2 values in the stable regions to design a suitable PLC.

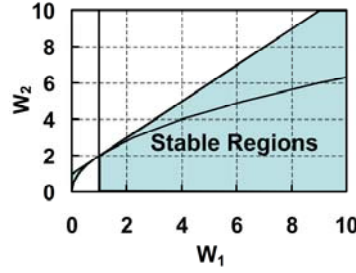


Figure 2.1. Stable regions of W_1 and W_2 for the PLC

2.2 Adaptive time delay estimator

The proposed PLC is based on a known time delay $\alpha\Delta t$; therefore, accurate estimation of delay is essential for delay compensation. In most hybrid tests, the time delay can be identified and assumed constant before the test. However, this delay could vary during the test especially when the specimen stiffness changes. As a result, the adaptive control theory is introduced to online estimate the time delay. In this study, the servo-hydraulic system is modelled by a second-order transfer function with only one unknown parameter α . Then a direct adaptive law is adopted to estimate the parameter. Finally, the gradient adaptive law is adopted in estimating the actuator delay using the parametric model.

The linear static parametric model (SPM) is obtained by separating the unknown parameters from the known signals. For example, the delay system with $W_1=3$ and $W_2=2$ in Eqn. 2.2 can be expressed as:

$$x_m[n] = x_m[n-1] + \frac{1}{\alpha} \left(\frac{3x_p[n] + 2x_p[n-1] + x_p[n-2] - 3x_m[n] - 2x_m[n-1] - x_m[n-2]}{6} \right) \quad (2.6)$$

where $x_p[n]$, $x_p[n-1]$, and $x_p[n-2]$ are the compensated displacements input to the servo-hydraulic system at the n th, $(n-1)$ th, and $(n-2)$ th step, The only unknown in Eqn. 2.6 is the delay step integer, α . By separating α from the known signals, the parametric representation is obtained by expressing the above system as a compact algebraic form:

$$\mu = \theta^* \phi \quad (2.7)$$

where θ^* is the unknown parameter. The parameters μ and ϕ are signals available from measurements by letting:

$$\begin{aligned} \mu &= 3x_p[n] + 2x_p[n-1] + x_p[n-2] - 3x_m[n] - 2x_m[n-1] - x_m[n-2] \\ \theta^* &= \alpha \\ \phi &= 6x_m[n] - 6x_m[n-1] \end{aligned} \quad (2.8)$$

The estimate of μ is generated by the estimation model which has the same form as the SPM except the unknown parameter θ^* is replaced with its estimated parameter, $\theta(t)$, i.e., $\hat{\mu} = \theta\phi$. It is expected that $\hat{\mu}$ approaches to μ when $\theta(t)$ approaches θ^* . However, the difference between $\theta(t)$ and θ^* is not available because θ^* is unknown. Therefore, the estimation error ε is obtained by the available measurements and defined as:

$$\varepsilon \equiv \frac{\mu - \hat{\mu}}{m_s^2} = \frac{\mu - \theta\phi}{m_s^2} \quad (2.9)$$

where $m_s^2 \geq 1$ is the normalizing signal designed to ensure that ϕ/m_s is bounded even when ϕ is not bounded. Generally, $m_s^2 = 1 + \phi^2$ is suggested.

The selected cost function can be expressed as:

$$J(\theta) = \frac{\varepsilon^2 m_s^2}{2} = \frac{(\mu - \theta\phi)^2}{2m_s^2} \quad (2.10)$$

The gradient method is used to minimize the cost function with respect to θ . The adaptive law based on the gradient algorithm takes the form:

$$\dot{\theta} = -\gamma \nabla J(\theta) = \gamma \varepsilon \phi \quad (2.11)$$

where γ is a scaling constant and referred as the adaptive gain.

It is noted that ϕ/m_s must be persistently exciting (PE). The PE condition requires that its integral over any interval of time is positive-definite. It is proved that the estimated time delay converges to the real time delay exponentially if the PE condition holds. However, most of the implementation of an online estimator or controller is often in digital form. It implies a discrete-time representation is required. A discrete-time parameter estimator can be derived by using a discrete-time approximation of the continuous-time one. More details of the approximation and the proof of parameter convergence can be found in the reference (Chen and Tsai 2012; Ioannou and Fidan 2006).

3. RESTORING FORCE COMPENSATOR

In this study, an on-line calculation procedure of moving-averaged tangent stiffness is developed to reduce the tracking error of the actuator. Consider a SDOF hybrid simulation using measured restoring force and analytically modelled inertia and damping forces, the equation of motion at time t is expressed as:

$$m_a \ddot{x}_c(t) + c_a \dot{x}_c(t) + k_{exp} x_c(t) = P_{eff}(t) \quad (3.1)$$

where $x_c(t)$ is the numerical integrated command displacement, and k_{exp} is the stiffness of the specimen. If the measured displacement, $x_m(t)$, is different from the command displacement, an error on the restoring force would occur and lead to an error in command displacement for the next step. As time goes by, these errors are accumulated and could even fail the test. It is well-known as error propagation. Hence, the error on the restoring force can be corrected using the following equation:

$$m_a \ddot{x}_c(t) + c_a \dot{x}_c(t) + k_{exp} x_m(t) = P_{eff}(t) - k_{exp} (x_c(t) - x_m(t)) \quad (3.2)$$

where $k_{exp}(x_c(t) - x_m(t))$ is defined as the restoring force compensator (RFC) to correct the error due to the difference between the command and the measured displacements. However, it is difficult to directly measure k_{exp} at each time step from a test specimen because the noise could be involved in the measurement. As a result, the moving-averaged tangent stiffness in discrete time is proposed. The

stiffness at the n th step, $k_{exp}[n]$ is computed by:

$$k_{exp}[n] = \frac{1}{T_0} \left(\sum_{k=n-T_0}^n \frac{f[k] - f[k-1]}{x_m[k] - x_m[k-1]} \right) \quad (3.3)$$

where T_0 is the number of samples used to calculate the moving-averaged tangent stiffness. The parameter $f[n]$ is the measured force at the n th step. If T_0 is too small, the calculated tangent stiffness would become sensitive to the measurement noise. On the other hand, if T_0 is too large, the calculated tangent stiffness could not represent the current stiffness change of the specimen.

However, in the very beginning of a test, the data before the current step are not available. In addition, the calculated tangent stiffness would become excessively large at the peak and valley displacements. As a result, the tangent stiffness is computed for three different stages at any given time t during the test: (1) when $0 \leq t \leq 2T_0 \Delta t$, k_{exp} is set as the elastic stiffness, k_e , (2) $2T_0 \Delta t \leq t \leq t_{ex}$, k_{exp} is obtained from Eqn. 3.3 but with the lower and upper bounds as $0 \leq k_{exp} \leq k_e$, where t_{ex} is the time duration of the ground accelerations, and (3) when $t_{ex} \leq t$, k_{exp} is set as k_e again.

4. NUMERICAL STUDIES

Simulink® was used to numerically investigate the feasibility of the proposed dual compensation strategy. All the numerical simulations were conducted using the same sampling rate of 1024Hz as the experimental facilities in the lab.

4.1 Delay estimator

Consider a first-order dominant hydraulic system with a 5Hz roll-off frequency, its transfer function is $31.42/(s+31.42)$. Convert the transfer function from continuous time to discrete time by using zero-order hold approach, the discrete transfer function with a 5Hz roll-off frequency is $0.03022/(z-0.9698)$. The weightings for the PLC were set as $W_1=3$ and $W_2=2$. The input excitation is a 120-second 1-mm sine sweep signal with a frequency content of 0.1 to 10Hz. The time history of the estimated delay is shown in Fig. 4.1. Apparently, the estimated delay converges to a value of 34 within 20 seconds. Figure 4.2 illustrates the time histories of the generated command, the compensated command, and the achieved feedback. There is a time delay between the generated command and the achieved feedback in the beginning. However, this time delay is shortened when the estimated time delay converges to $\alpha=34$. It indicates that the proposed adaptive PLC is self-tuning during the test and then compensates the servo-hydraulic system online properly. Moreover, since the poles of the proposed PLC are always within a unit circle. Thus, the stability of the overall system is proved.

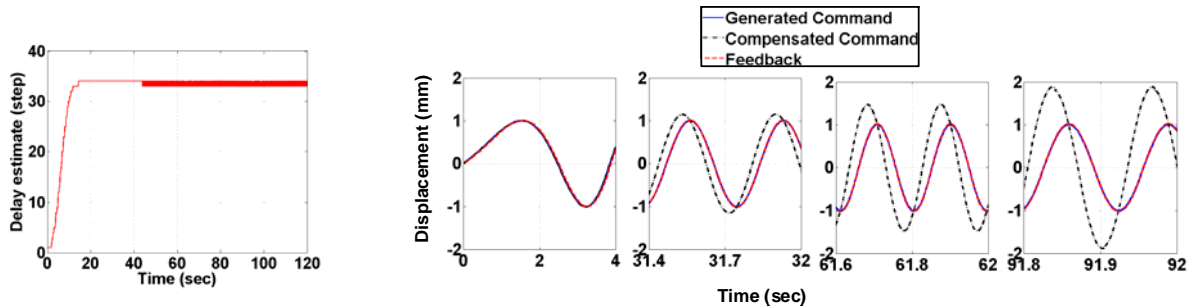


Figure 4.1. Time history of delay estimate

Figure 4.2. Time history of generated command, compensated command and feedback

4.2 Real-time hybrid simulation for inelastic structures

An SDOF shear building model was considered to evaluate the proposed delay compensation. The

structural period is 0.5 second and the damping ratio is 2%. The structural mass, damping coefficient and stiffness are 30000 N-s²/m, 15080 N-s/m and 4737410 N/m, respectively. The restoring force was measured from a determined 10-step-delay specimen and sent back to the integration algorithm to calculate the target displacement in the next time step. The ode solver of MATLAB using Forward Euler integration algorithm was adopted in the simulations. Again, $W_1=3$ and $W_2=2$ were used for the PLC. The Bouc-Wen model (Wen 1976) was used to represent the nonlinear hysteretic response of the structural system. The restoring force, $F(t)$, can expressed as:

$$F(t) = ak_u u(t) + (1-a)k_v v(t) \quad (4.1)$$

where a is the ratio of post-yield to elastic stiffness. $v(t)$ is the hysteretic variable:

$$\dot{v}(t) = A\dot{u}(t) - B|\dot{u}(t)||v(t)|^{\eta-1}v(t) - C\dot{u}(t)|v(t)|^\eta \quad (4.2)$$

where A , B , C , and η are parameters that determine the scale, general shape, and smoothness of the hysteretic loop. In this study, $A=1$, $B=300$, $C=200$, $\eta=1.5$, and $a=0.02$ were used for the simulations. A 50-second 1999 Chi-chi near-fault Earthquake record (TCU068EW) normalized to a PGA=0.2g was used as the input excitation. The duration of the structural responses was 60 seconds including a 50-second earthquake excitation and a 10-second free vibration. The response of the same structure without delayed restoring force is viewed as the exact solution. There were two cases of analytical simulations: the system was compensated by (1) the adaptive PLC only (PLC), and (2) the PLC and RFC (PLC+RFC). The analytical simulation results were compared with the exact numerical solution (denoted as Exact). Figure 4.3 shows the displacement time histories of the simulation result and the exact solution for the nonlinear structure. The structural displacements are larger than that of the Exact in the beginning because it takes more than 12 seconds for the delay estimator to converge to the system delay. After the delay estimate converges, the overall system becomes stable. The hysteresis responses for the compensated system and the exact solution are shown in Fig. 4.4. Evidently, the two curves agree with each other rather well. Thus, it is confirmed that the proposed PLC improves the system stability by compensating the system delay appropriately. Figure 4.5 shows the accumulated displacement error of the two analytical simulations. The accumulated displacement error is defined as:

$$Error_{ac} = \sum_n \text{abs}(x_m[n] - x_{exact}[n]) \quad (4.3)$$

where $x_{exact}[n]$ is the displacement of the exact solution at the n th step. The accumulated error of using PLC only is much larger than that of using PLC+RFC.

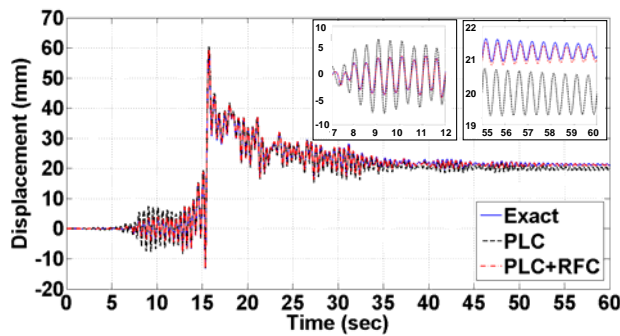


Figure 4.3. Analytical displacement time histories of an inelastic system

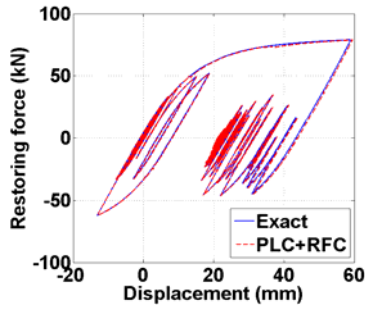


Figure 4.4. Hysteresis loop of the inelastic simulations

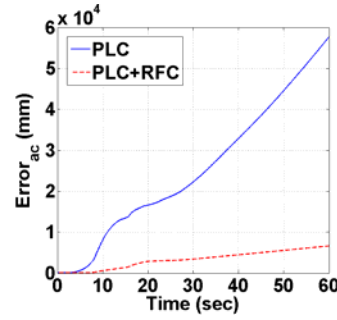


Figure 4.5. Accumulated displacement error time histories

5. EXPERIMENTAL STUDIES

A schematic of a substructuring experiment is used to validate the proposed compensation strategy. The system is divided into two parts: (1) the experimental substructure, consisting of the spring represented by a steel plate anchored between a shaking table and a rigid frame, and (2) the numerical model, consisting of the damping and the mass. The overall test setup is shown in Fig. 5.1. The table top is made from a stiffened aluminum plate with tapped holes for mounting the fixtures and specimen. The dimension of the A36 steel plate specimen was designed as 630mm high by 250mm wide by 10mm thick. Two 300mm long 120×120×12mm steel angles are used to clamp the steel plate using 12 high-tension bolts on both top and bottom edges of the specimen. In this example test, the stiffness term in the equation of motion is completely determined from the test specimen. This configuration is considered as one of the most challenging cases for conducting a real-time hybrid test as the accuracy of the test is highly dependent on the accuracy of the imposed displacement and the restoring force measurement.

The entire test facility, as shown in Fig. 5.2, can be divided into two major components: (1) the MTS GT digital controller, and (2) the xPC host-target pair. The GT digital controller is a real-time controller that provides the closed loop control of the system. The update rate of the GT digital controller is 1024Hz. A Shared Common Random Access Memory Network (SCRAMNet) interface for the GT controller is provided to allow hybrid testing capabilities. The xPC target is an environment where the host and target computers are two different desktop computers. One of the desktops is used as a host computer with the Matlab/Simulink to create the control model using Simulink blocks. With Real-Time Workshop and C compiler, executable codes can be created and linked to the second desktop which runs in real time with a SCRAMNet card to connect to the GT controller. Signals are passed between the GT controller and the xPC target in digital form over the SCRAMNet through the optical cables. In the experimental studies, a PI controller was used as the closed loop feedback controller.

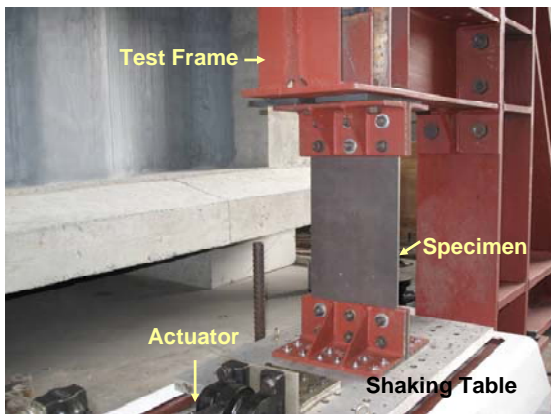


Figure 5.1. Experimental setup

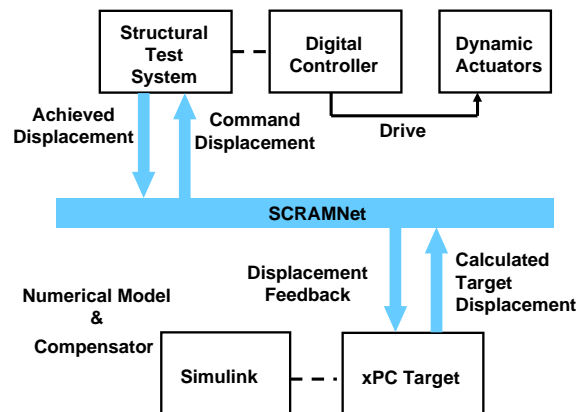


Figure 5.2. Hardware layout of the control system

An initial time delay integer $\alpha=17$ was used after conducting system identification tests of the servo-hydraulic system. The preliminary parameters for the PLC are $\alpha=17$, $W_1=3$ and $W_2=2$. The mass of the shaking table and the fixtures (45kg all together) induced the inertia force, which was included in the actuator end load cell measurement. Moreover, it was observed that the friction and viscous forces were highly nonlinear, depending on the table velocity and displacement. As a result, the analytical model of the benchmark is considered the combined effects of the restoring, friction, viscous forces and the inertia force. In this study, the numerical simulation result of the calibrated benchmark is considered as the exact solution of the real-time hybrid tests.

Another important issue is the T_0 values adopted in computing the moving averaged tangent stiffness for the RFC in Eqn. 3.3. Three different T_0 values were tested to seek the appropriate number of samples in computing the moving-averaged tangent stiffness. They were (1) $T_0\Delta t=0.2T$ (2) $T_0\Delta t=0.1T$, and (3) $T_0\Delta t=0.05T$, where T is the fundamental period of the SDOF structure. Figure 5.3 illustrates the schematic of the proposed dual-compensation strategy in the experimental studies.

A 30-second 1940 El Centro Earthquake was adopted for the real-time hybrid tests. For comparison purposes, the PGA was normalized to 0.04g and 0.02g for the 0.5-second and 1.0-second period SDOF structures, respectively. These two structures were expected to have similar peak displacements. The elastic stiffness, 666400 N/m, is obtained by the elastic test. Hence, the corresponding mass and damping coefficient of the two structures are shown in Table 5.1. The duration of a real-time hybrid testing was 40 seconds including a 30-second earthquake excitation and a 10-second free vibration. Figure 5.4 shows the time histories of each test and the benchmark response for the $T=0.5$ second case. It is evident that all the test responses are close to the assumed exact solution except the one used the PI feedback controller without compensation. However, the responses of $T_0\Delta t=0.05T$ case are not very consistent with the assumed exact solution when the response is small. This is because in the case of small $T_0\Delta t$ value, the system friction forces became more disturbing for computing the tangent stiffness when the structural displacements and restoring forces were small. On the other hand, the test results fit the assumed exact solution rather well when $T=1.0$ sec. as shown in Fig. 5.5. The differences between each test and the benchmark are less than 0.8mm even when the displacements are small. In particular, the responses of $T_0\Delta t=0.05T$ are rather consistent with those of the other tests. The effects due to nonlinear friction force are not obvious.

Figure 5.6 shows the delay estimates of each test of the two SDOF structures. Apparently, the delays vary within 16 to 19 steps during the test. The variation of the delay estimates is considered not so significant. Thus, if a 17-step constant delay PLC is adopted in the tests, test results should be still stable and acceptable. Figure 5.7 shows the varying tangent stiffness calculated in each test. When the structural responses are small, the computed tangent stiffness is zero due to the prescribed lower bound limit. It implies that there must be significant noises from the viscous and friction forces of the shaking table especially when the displacements are small. These noises have resulted in unreasonable results of the computed tangent stiffness. In the case of $T=1.0$ sec., the computed tangent stiffness is bounded to zero because the structural responses are mostly smaller than 2mm. A lower bound of zero indicates that the RFC is completely excluded from the compensation strategy during the small response time regions. This helps to explain that the three test responses in the case of $T=1.0$ sec. are similar. Thus, the proposed tangent stiffness boundaries seem appropriate to prevent an erroneous compensation computed from unexpected tangent stiffness spikes. The RFC being zero also confirms that only the outer-loop PLC is sufficient to compensate the delay system when the structural responses are small.

Table 5.1. Structural properties of the SDOF structures in the validation tests

Structural Period (sec)	Mass (N-s ² /m)	Damping Coefficient (N-s/m)	Stiffness (N/m)
0.5	4220	2121	666400
1.0	16880	4242	666400

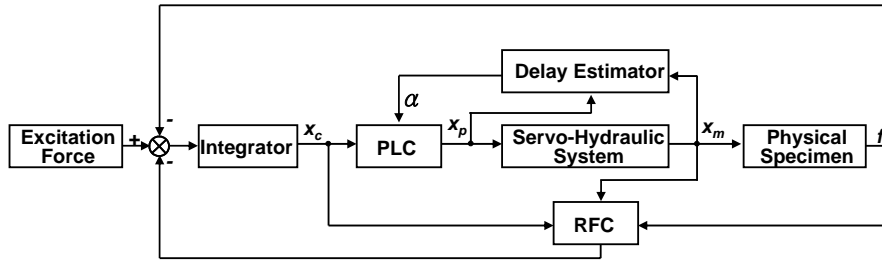


Figure 5.3 Block diagram of the dual compensation strategy in the experiments

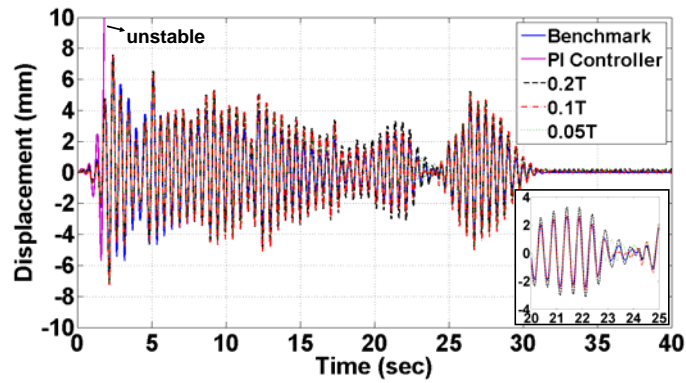


Figure 5.4 Experimental and analytical results ($T=0.5\text{sec}$)

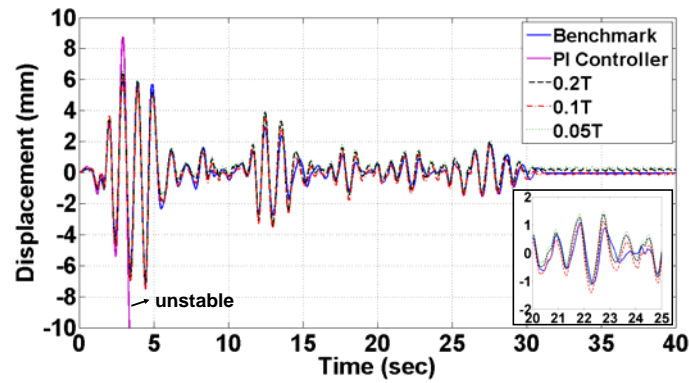


Figure 5.5 Experimental and analytical results ($T=1.0\text{sec}$)

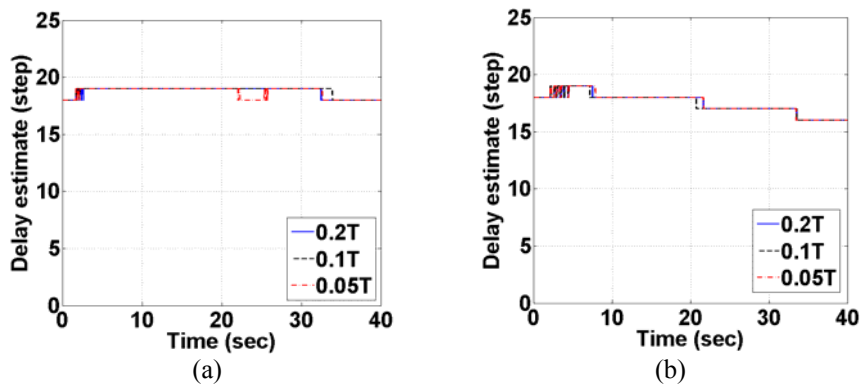


Figure 5.6 Time histories of the delay estimate (a) $T=0.5\text{sec}$ (b) $T=1.0\text{sec}$

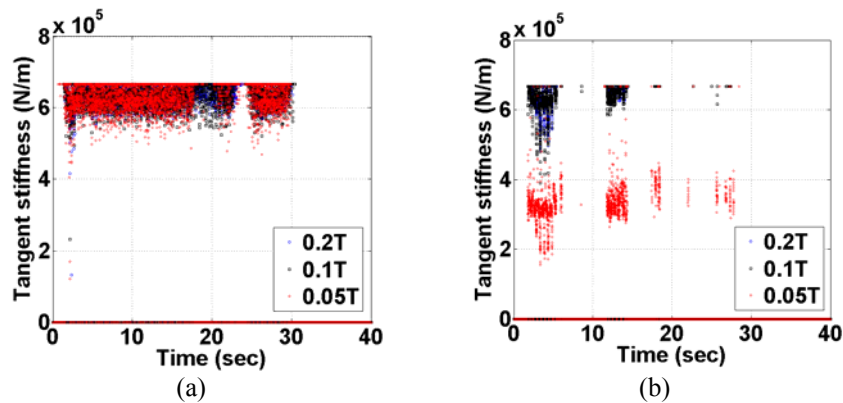


Figure 5.7 Time histories of the tangent stiffness (a) $T=0.5\text{sec}$ (b) $T=1.0\text{sec}$

6. CONCLUSIONS

A dual-compensation strategy based on the inversed transfer function and the force balance of the equation of motion has been proposed. It is a combination of displacement and force compensation. The delay estimator based on the gradient adaptive law is adopted to estimate the delay during the test. For numerical studies, simulation results indicate that the proposed PLC with delay estimator compensates the delay system rather well as long as a proper adaptive gain is tuned. In addition, the accumulated displacement error of the dual-compensation method is significantly reduced compared with that of using the PLC only. For experimental studies, a one-tenth structural period of sampling number is suggested as the test results demonstrate favorable agreements with the benchmark responses. Besides, the stiffness lower bound successfully prevented the RFC from unreasonable compensation and resulted in a stable zero compensation.

AKNOWLEDGEMENT

The authors would like to thank the technicians from National Center for Research on Earthquake Engineering in Taiwan for their assistance in test setup. In addition, the sharing of the dynamic shaking table from National Taiwan University is much acknowledged.

REFERENCES

- Horiuchi, T., Inoue, M., Konno, T. and Namita, Y. (1999). Real-time hybrid experimental system with actuator delay compensation and its application to a piping system with energy absorber. *Earthquake Engineering and Structural Dynamics* **28:10**, 1121–1141
- Zhao, J., French, C., Shield, C. and Posbergh, T. (2003). Considerations for the development of real-time dynamic testing using servo-hydraulic actuation. *Earthquake Engineering and Structural Dynamics* **32:11**, 1773–1794.
- Jung, RY. and Shing, PB. (2006). Performance evaluation of a real-time pseudodynamic test system. *Earthquake Engineering and Structural Dynamics* **25:4**, 333–355.
- Chen, C. and Ricles, JM. (2009). Improving the inverse compensation method for real-time hybrid simulation through a dual compensation scheme. *Earthquake Engineering and Structural Dynamics* **38:10**, 1237-1255
- Darby, AP., Williams, MS. and Blakeborough, A. (2002). Stability delay compensation for real-time substructure testing. *Journal of Engineering Mechanics* **128:12**, 1276–1284.
- Ahmadizadeh, M., Mosqueda, G. and Reinhorn, AM. (2008). Compensation of actuator delay and dynamics for real-time hybrid structural simulation. *Earthquake Engineering and Structural Dynamics* **37:1**, 21-42.
- Chen, PC. and Tsai, KC. (2012). Dual-Compensation Strategy for Real-time Hybrid Testing. *Earthquake Engineering and Structural Dynamics* DOI: 10.1002/eqe.2189.
- Ioannou, PA. and Fidan, Barış. Adaptive Control Tutorial. (2006) Society for Industrial and Applied Mathematics, Philadelphia
- Wen, YK. (1976). Method for random vibration of hysteretic systems. *Journal of Engineering Mechanics* **102:2**, 249-263.